

GLACIAL LAKES EXTRACTION IN SENTINEL-1 SAR GRD DATA USING RESIDUAL ATTENTION U-NET++ MODEL

MAHESWARAN T^{1*}, Cyril Mathew O²

^{1*}Part Time Research Scholar, M P NACHIMUTHU M JAGANATHAN ENGINEERING COLLEGE, CHENNIMALAI ERODE 638112.
tmaheswaran411@gmail.com

²Professor/ECE, Al -Ameen Engineering College, Erode 638104. cyrilmathew15@gmail.com

Corresponding id: tmaheswaran411@gmail.com

Abstract

A crucial component of the cryosphere in the the Karakoram range of mountains are glacier lakes. Glacial lake outbursts floods (GLOFs) pose a short-term hazard to downstream communities and ecosystems due to rising temperatures caused by climate change. As a result, monitoring GLOF dangers requires the use of the Glacial Lake map method. Data from the Sentinel-1 Ground Range Detected (GRD) microwave mission were used in this analysis. Regardless of the weather or cloud cover, it can penetrate and use dual polarization (HH + HV or VV + VH). The purpose of this research is to examine how algorithms based on machine learning may be used to extract water bodies from GRD data and how effective they are. Supervised Machine Learning classifiers and GRD backscattering analysis form the backbone of the research methodology. Common deep learning methods include FCN, U-Net, U-Net++, and others. The suggested Residual Attention U-Net++ model in this research makes use of both extraction maps and attention maps. In the research region, both approaches provide superior results for mapping glacial lakes. However, when it comes to total backscattering analysis, the mean backscatter parameter has the greatest accuracy rate. The classification method also included comparing each classifier's output to the reference data to determine its correctness. In order to ascertain the brief flood outburst and implement future preventative measures, the high precision of classification achieved while extracting glacial lakes utilizing our method will prove valuable.

Keywords: Sentinet-1 GRD; Residual Attention U-Net++; Himalaya Glacial Lake Extraction; Super Pixel Segmentation; Data Augmentation

1. INTRODUCTION

Manual field surveys are arduous, costly, and time-consuming ways to determine the outburst vulnerability of glacier lakes. Consequently, in order to efficiently extract glacial lakes from satellite data, a trustworthy and autonomous system is

needed. The main obstacles to gathering data on the area around the glacier lake are the satellite pictures' uneven backgrounds and low spectral contrast [1]. In order to assess the potential for glacial lake eruptions, it is essential to extract lake areas from satellite pictures. The majority of the methods that have been mentioned thus far depend significantly on labor-intensive, costly, and time-consuming field surveys. Consequently, the precise extraction of glacial lake regions from satellite data necessitates a reliable and autonomous system. Extracting information from Landsat8 satellite pictures in the glacier lake region is very challenging because to the low contrast and varied backgrounds [2]. A large number of glacial lakes, particularly in Tibet's southeastern region—the main concentration region for marine-type glaciers—are very vulnerable to the effects of climate change. While glacial lakes are vital to the region's freshwater ecosystems, they also threaten local communities and infrastructure with devastating floods when they break [3].

In order to detect and avoid glacial lake catastrophes, remote sensing tracking of these bodies of water is crucial. While current methods for extracting glacial lakes from Landsat images have shown impressive results, the algorithms used to do so aren't equipped to handle the unique spectral, shape, and texture characteristics of glacial lakes, and they necessitate human intervention in the form of design parameters in order to automate their optimization [4]. In the south of Tibet, glacial lakes provide a significant supply of freshwater. Nonetheless, locals' safety has been seriously compromised by floods caused by glacial lake outbursts. The areal fluctuations in glacial lakes need to be evaluated over the long period with the help of local data if we want to know how these lakes are changing as a result of climate change [5]. For the purpose of identifying changes in water supplies and possible dangers in alpine cryospheric zones, it is crucial to continuously monitor and record the fluctuation of glacier lakes. There is a lot of subjectivity and inefficiency in the present semi-automated glacier lake mapping approaches [6]. An efficient method of tracking the spread of bodies of water and eruptions is the remote sensing extraction of glacier lakes. Imperfect precision and erroneous glacier lake outlines are now the result of

semantic segmentation networks' edge identification difficulty and a dearth of resources pertaining to glacial lakes [7].

Since GLs affect snowmelt runoff, stream flow, water resources, and GLOF (glacial lake outburst flood), tracking their regional and temporal variations is crucial against the backdrop of continuing climate change. When multi-year time-series analysis is taken into account, however, accurately identifying and mapping GLs in the backdrop of snow-clad mountains by visual interpretation of satellite imagery is a tough and arduous undertaking [8]. Changes to the Tibetan Plateau's glaciers while glacial lakes due to climate change need a thorough assessment. A typical monsoonal marine glacier region, the Southeastern Tibetan Plateau is very susceptible to the effects of climate change. Humid and warm currents from the Indian Ocean impact it [9]. Glaciers in high-mountain regions across the globe are undergoing a dynamic metamorphosis due to climate change-induced recession. As a consequence, glacial lakes are formed, grow, and eventually disappear, which might endanger people downstream and highlights the need of constant monitoring [10].

This research intends to establish an automated, accurate, and robust glacial lake mapping strategy that is not constrained by weather conditions, cloud cover, or complexity of mountainous terrains. The broad aim of this project is to use Sentinel-1 SAR GRD data in combination with machine learning algorithms by improving the glacial lake mapping through the disasters of the proposed Residual-Attention UNet++ where it has used attention mechanisms, residual units, and dense skip connections in order to improve feature learning, minimize the semantic gap and minimize the model's ability to detect everything that is not a water body. This ensures reliable detection of water bodies even in challenging cryospheric environments. The aim of this research is a response to the increasing danger of glacial lake outburst floods (GLOFs) resulting from accelerated glacier melting due to climate change. Communities downstream of the Karakoram range and similar high-altitude areas are at considerable risk, emphasizing the need for timely, consistent, and high-resolution monitoring of glacial lakes. Furthermore, existing methods using optical methods are often constrained by cloud cover, In addition, data availability is inconsistent. SAR imagery can be obtained in all-weather conditions and day or night, therefore permanent monitoring is feasible. The scope of this work done by encompasses many test sites across High Mountain Asia, the Alps, and the Andes, supporting potential application of the model and the research in diverse topography options. The project also involved standardizing the preprocessing workflows we used for the SAR data processing. We were also able to identify niche techniques for orbited file correction, thermal and border noise removal, calibration, speckle filtering, and terrain correction. This model and workflow will

introduce a robust preprocessing and deep learning combined approach and a globally scalable and potentially transferable and open-source solution for large-scale monitoring of the cryosphere. In the end, the goal of these frameworks and from the materials used is to develop platform that contributes to early warning systems, disaster preparedness, and responsible resource management in vulnerable mountainous communities.

The following is an overview of the main points made by this work:

- UNet++ was updated with the addition of the attention mechanism and residual unit to address the degradation issue and boost the weight of goal regions.
- For the purpose of glacial lakes picture segmentation, the Residual-Attention UNet++ model was presented.
- Results showed that experimental techniques outperformed state-of-the-art approaches in segmentation tasks on three different glacial lakes imaging datasets.
- Residual-Attention UNet++ has the ability to improve the segmentation job by giving more weight to the target region and suppressing the background area that is unimportant.
- Outperformed other UNet-based algorithms in a comparison.
- With little performance hit, the trimmed Residual-Attention UNet++ allowed for quicker inference.

This is how the rest of the material is structured. Following an overview of relevant literature in Section 2, this article introduces its suggested designs in Section 3, specifies the datasets, experiments, and findings in Section 4, and ultimately draws conclusions in Section 5.

2. RELATED WORK

Based on microwave Sentinel-1 SAR GRD data [16]. It has the potential to dual-polarize (HH+HV or VV+VH) and penetrate clouds and other meteorological conditions. This study suggests a method for analyzing GRD data and to evaluate the accuracy of machine learning algorithms for water body identification. Important to the study technique are GRD backscattering analysis and supervised Machine Learning classifiers. ML methods are more effective than the other when it comes to mapping glacial lakes in the study area. On the other hand, the mean backscatter factor yields the most accurate results in total backscattering study. As part of the classification process, we checked the accuracy of each classifier by comparing their results to the reference data. Their approach was able to accurately extract glacial lakes, which will aid in the prediction of when floods would occur and in the development of strategies to mitigate such disasters. Researchers in the

Hindu Kush, Karakoram, and Himalaya (HKKH) region looked at the feasibility of mapping glacier lakes using PlanetScope pictures in [17]. Although the PlanetScope photos have a quick return time, thanks to 130+ small satellites, the imaging sensors on board these spacecraft have varied spectrum sensitivities and decreased dynamic range, limiting the imagery to four bands. The water pixels' different spectral fingerprints induced by differences in composition, turbidity, and depth, as well as cast shadows in hilly places, make it challenging to automatically and reliably extract surface water in PlanetScope pictures. While keeping these constraints in mind, the work uses cutting-edge deep learning models to pixel-by-pixel categorize PlanetScope photos as either water or backdrop. We then compare these findings to those of Random Forest using SVM classifiers. The DL model avoids most of the aforementioned problems was proposed by the authors of [18] for accurately identifying and mapping glacial lakes using multi-source data and machine learning techniques such as the random forest classifier algorithm. This dataset is a compilation of information gathered from many sources, such as Sentinel-1 radar backscatter and Sentinel-2 radar near-field interference (NDWI). In order to determine the best way to partition potential glacial lakes, they input these data into an expert system. The method's effectiveness was assessed at eight separate test locations distributed throughout various Alpine regions. The Tajiks Pamirs, the Peruvian Andes, the Swiss Alps. The results show that the proposed method is applicable to a wide range of geographical, geologic, climatic, and glacial lake situations. The authors of [19] helping with the concept creation phase of the project and have outlined the expected methodological steps as well as provided some early results. They locate potential future lake emergence sites and get basic information such as volume, depth, and elevation distribution using recently disclosed data on the distributions of glacial ice thickness around the world. For every mountain range on Earth by comparing the percentage of present glacial lakes to that of future glacial lakes, and they use a recently-compiled global inventory of glacier lakes for this. Together with a worldwide glacier development model, they foretell when these future lakes will be formed, supposing different RCPs. Their first objective will be to assess the area for any potential risks or threats. By analyzing the topography around each possible lake to the impacts of mass movement is assessed in a broad sense. The potential impact on subsequent processes will be evaluated by use of elementary flow routing models.

In this work, researchers from the HKH region of Pakistan evaluated the risk of a glacial lake outburst flood using ground information [20]. The present study identified 30,44 lakes covering a total of about 134.8 km² throughout the three HKH mountains. With 1,325 lakes, the Karakoram range has the most, while the Hindu Kush range had the fewest, at 722. The region's size increased by 7% and the number of lakes by about 26%. There was a 91% rise in the number of lakes between 2500 and 3500 meters, a 20% increase between 3500 and 4500 meters, and a 31% increase between 4500 and 5500 meters. A

minimum of 36 lakes discovered in the HKH region in 2013 were identified as PDGLs, or potentially dangerous glacial lakes; hence, these lakes have the potential to trigger GLOFs. The ESA Sentinel-1 GRD time series data model was developed by the authors of [21] using the Google Earth Engine API with the purpose of monitoring floating rubbish in lake areas. Finding the optimal method for monitoring floating debris caused by rains is the primary objective of the research. In order to manage water resources while maintaining water quality, it is necessary to regularly monitor floating debris from multifunctional dams from the early generation stage onward. This study's bodies of water were simply identified using a Synthetic Aperture Radar time-series assessment approach, which was developed in response to the low accessibility over broad areas. Though SAR satellite pictures might be used to investigate aquatic environments inside, no studies have focused on identifying trash on water surface surfaces. For the first time, areas of floating debris were discovered in many lakes using GRD photos acquired by the ESA's Sentinel-1 satellite, according to that study. Differentiating them from natural objects, such as invasive floating plants, was shown. The condition at Daechong Dam is described in that report. Following heavy rain, floating debris was located using Sentinel-1 SAR GRD data. Finding various kinds of floating trash that might wind up in drinking water dams and organizing future collections could benefit from this.

2.1 Research Gaps

The growth and evolution of glacial lakes must be continuously monitored in order to control and mitigate the risks associated with these GLOFs. To monitor and map glacier lakes, geospatial techniques and remote sensing satellite imagery have been used often because of the difficult and inaccessible terrain. Traditional approaches to analyzing remote sensing pictures for the purpose of identifying spectral and textural properties of glacier lakes rely significantly on human involvement. An efficient method of tracking the spread of bodies of water and eruptions is the remote sensing extraction of glacier lakes. Currently, semantic segmentation networks have trouble with edge identification and there aren't enough glacial lake datasets, so the results aren't very reliable. This approach excels at refined outline identification and tiny glacier lake extraction; it may be used to extract glacial lakes from high-resolution pictures in the high-Asia area. By analyzing the prediction matrices, we were able to determine that the U-Net model had an outstanding value. So, the research proves that U-Net is a great tool for finding glacial lakes quickly and keeping an eye on them.

The proposed Residual-Attention UNet++ was chosen because it resolves some of the significant limitations currently seen in existing methods, such a requiring an expert to tune the parameters and having limited accuracy when well-made an when tested using imagery collected during challenging terrain and atmospheric conditions. Rather than being a traditional

classifier model, our model utilizes attention gates, residual units, and dense skip connections to incorporate all relevant information from the image to build up complex glacial lake features, which existing methods currently fail to provide accurate segmentation. The proposed integrated structure substantially improves segmentation accuracy and segmentation robustness. The proposed model effectively segments features in all weather conditions because it only utilizes all-weather Sentinel-1 SAR GRD data, which ensures it is performing reliably without concerning about clouds Content. Together these properties make the Residual-Attention UNet++ model for cryosphere monitoring much more relevant than previous approaches.

3. SYSTEM MODEL

Preprocessing GRD data obtained from the Copernicus Sentinel-1 mission was described in the study using a typical generic procedure. One goal of the method is to produce preprocessed Sentinel-1 SAR GRD data. With this data as a foundation, further products as well as operational downstream services may be developed with consistent Copernicus Sentinel-1 SAR GRD data. Common changes made by the technique include ensuring an exact acquisition orbit, removing noise from thermal pictures and boundaries, calibrating the radiometric system, using range Doppler, and correcting for terrain. Sentinel-1 Synthetic Aperture Radar (SAR) data has a high return frequency and improved spatial resolution, making it very adaptable. Even while Sentinel-1 SAR GRD data with few changes is suitable for study, a wider range of users need products with an accepted set of corrections created. To make Sentinel-1 SAR GRD products easier to use, standardizing approaches to data preprocessing is essential. This general standard approach may be used to preprocess data from the Copernicus Sentinel-1 SAR GRD mission. As mentioned in the procedure, some of the objectives are to calibrate the radiometric sensor, eliminate border noise in thermal and pictures, set up an accurate acquisition orbit, apply a variety of standard corrections, and compensate for range Doppler and terrain. To further encourage the adoption of data fusion methods for virtual constellations with satellites, the technology also makes it easier to spatially snap Sentinel-1 SAR GRD inputs to Sentinel-2 MSI information grids. Following the provided procedure, one may generate a collection of Sentinel-1 SAR GRD data that has been preprocessed. Using consistent Copernicus Sentinel-1 SAR GRD datasets, this data may then be used as a standard for future product and operational downstream service development. Ultimately, we want to make sure that many communities have access to reliable information. The overall objective of this project is to develop a method and Python package called "GLakeMap" that can map glacial lakes independent of factors such as cloud cover, geographic location, weather, and lake characteristics. The purpose is accomplished by the integration of the Sentinel-1 Synthetic Aperture Radar (S-1 SAR). We test our automated technique on each location. The following areas are potential

locations for HMA tests: the Boshula mountain range to the southeast of the Tibetan Plateau, Bhutan to the east, the Koshi basin to the center, the state of Jammu and Kashmir to the west, Tajikistan close to central the Pamir Mountain Range, and the countries of Turkmenistan and Kazakhstan in northern Tien Shan.

3.1 Data Acquisition

Data accessibility and availability entered a new era with the introduction of the European Commission's Copernicus Programme. The program aimed to provide six themed services using data gathered from Earth observation satellites and in-situ observations. The Copernicus Programme has become the world's largest source of space data by making accessible, without charge, all satellite data—primarily acquired by Sentinel spacecraft. Sentinel data is useful for various applications because to its higher return frequency and improved geographical resolution.

Two polar orbiting satellites, Sentinel-1A and Sentinel-1B, are part of the Sentinel-1 mission. They can take pictures in all lighting or weather circumstances thanks to a C-band synthetic aperture radar technology that uses a core frequency of 5.405 GHz. Synthetic Aperture Radar data with single or dual polarization and a 6-day return duration is gathered by Sentinel-1 satellite constellations.

Sentinel-1 SAR GRD uses an Earth ellipsoid framework to provide products that include several process that focused SAR data. This information is needed to alter the ellipsoid projection of the GRD products; as mentioned in the product generic annotations. Square pixels in the Sentinel-1 SAR GRD image have reduced speckle and represent just the measured amplitude; phase information is removed as a result of the multi-look processing. The height of the landscape is supplied by the general annotation that is a consequence of adjusting the ellipsoid projector of GRD products. The range stays the same, although the terrain's height could shift in any given direction.

The concept of ground range coordinates is derived from slant range coordinates that are projected onto the ellipsoid of the Earth. The values of the pixels stand for the magnitude that was really seen. There is a lack of phase data. Reduced speckle, square pixel spacing, and approximately square spatial resolution are the outputs of the multi-look processing.

A data collection of noise vector annotations, which include thermal noise vectors, is part of the product annotations. The noise may then be removed from the power detected image, enabling users to perform thermal noise correction. One application that may aid in the reduction of thermal noise is the Sentinel-1 Toolbox. Depending on the acquisition technique and degree of multi-looking, GRD products may have three

different resolutions: Full Resolution, or Good Resolution, and Moderate Resolution.

3.2 Preprocessing

Data from the Copernicus Sentinel-1 SAR GRD mission may be preprocessed using this standard generic methodology. All of the Sentinel satellite toolboxes have a similar architecture called the Sentinel application framework, which is where the workflow was developed. Sentinel-1 SAR GRD may be processed with the command line graph processing paradigm with a 'xml' processing graph, which enables batch processing of big datasets.

Each of the seven processing stages that make up the pretreatment workflow is detailed in its own paragraph with the goal of minimizing the likelihood of error propagation in the next phases.

a. Apply Orbit File

Including incorrect orbit state vectors in the metadata of SAR products is typical practice. The product is prepared a few days after precise satellite orbits are acquired, and they are made available a few days to weeks later. Each SAR scene's product metadata may dynamically download and update the orbit condition vectors using SNAP's exact orbit operation, providing precise details about the satellite's location and velocity.

b. Thermal Noise Removal

Specifically, the Sentinel-1 image intensity is impacted by cumulative thermal noise in the cross-polarization channel. By reducing discontinuity among sub-swaths and leveling the backscatter signal over the complete Sentinel-1 image, thermal noise reduction, in multi-swath collection modes, minimizes the impacts. In SNAP for Sentinel-1 data, the temperature reduction of noise operators could restore signals that were removed during level-1 product creation, modify products annotation to reflect this change, and then apply the correction once again. To generate corrected noisy profiles that correspond to the calibrated GRD data, one uses the noise look-up table provided by Sentinel-1 level-1 output in linear power.

c. Border Noise Removal

When creating level-1 items, it is essential to adjust the specimen start time to account for the change in Earth's curvature. Because of compression in both azimuth and range, radiometric artifacts show up around the picture's periphery. To eliminate low-level noise and erroneous data around scene borders, SNAP's border noise reduction operator was created. Figure 1 shows the flowchart of the preprocessing system.

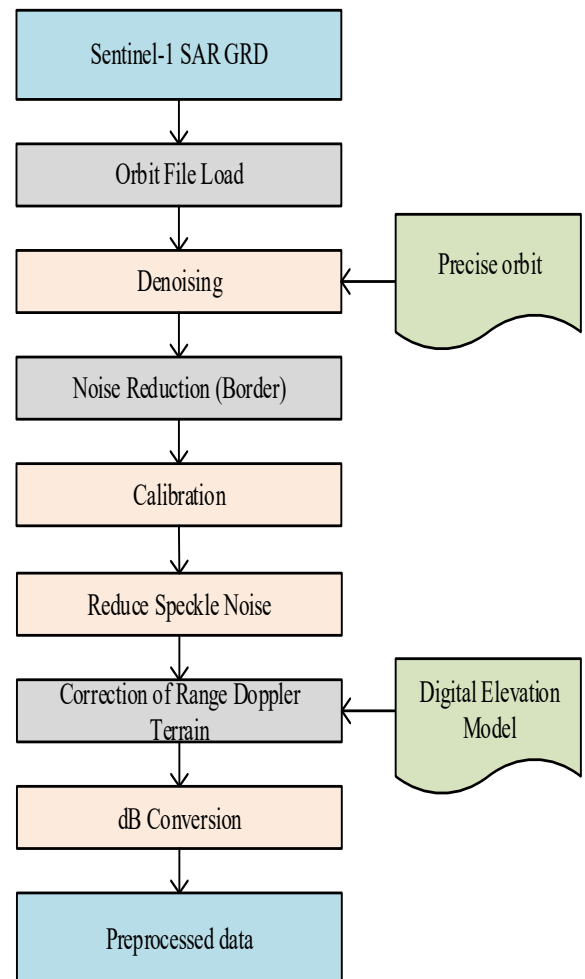


Fig.1. Data Preprocessing Flowchart

d. Calibration

The measuring process creates radiometrically calibrated SAR backscatter by converting digital pixel values. A calibration vector is added to the Sentinel-1 SAR GRD product so that the calibration equation can be executed. This vector makes it simple to convert image intensity data into sigma nought values. Throughout the measurement, a range-dependent gain and a constant offset are applied, one of which is the absolute calibrating constants. The scaling factor that was used to produce the level-1 product is now inverted. In order to produce SAR backscatter that has been radiometrically calibrated with regard to the nominally horizontal plane, the suggested pre-processing step includes a LUT that produces sigma nought values. While the strength of reflected is determined by the geometric crossing section of a transmitting sphere, sigma is the radar cross section of a scattered target in comparison to what would be expected from a one square meter region. The parameters of the reflecting appear, the wavelength, polarization, and incidence angle are some of the variables that influence the sigma nought.

e. Speckle Filtering

The granular noise that appears as speckle in synthetic aperture radar images is actually the consequence of wave interference from a number of simple scatterers. Using speckle filtering is one method of enhancing picture quality. By doing this action early in the SAR data processing process, speckle is kept from spreading to later procedures (such as dB conversion or terrain correction). Speckle filtering is not advised for scenarios where identifying fine-grained spatial structures or picture texture is crucial because it may remove information on these aspects. The enhanced Lee filter performs better than competing then other filters for visual interpretation. This is because, in comparison to its rivals, it stores more information about textures, point targets, and edges. The multitemporal speckle filter is a more recent method of speckle reduction that uses several SAR measurements over time. You can select "None" as the filter type if you wish to omit the speckle filtering step from the recommended pre-processing approach.

f. Range Doppler Terrain Correction

For the most part, while sensing SAR data, the viewing angle is larger than zero degrees, which causes some distortion in the pictures due to the geometry of side-looking. The goal of applying terrain adjustments is to eliminate these artefacts and make the geometric depiction of the scene seem as accurate as feasible. Foreshortening and shadows are among the geometric distortions caused by topography that range Doppler terrain correction removes by using a digital elevation model to adjust each pixel's positioning. To get the exact geolocation data, it makes use of the orbit state vector data that is already included in the metadata, the radar frequency annotations, the space-to-ground conversion parameters, and the reference data from the digital elevation model. The operator allows you to select the photo resampling method and the pixel spacing of the target CRS. This processing phase allows the spatial snapping of Sentinel-1 SAR GRD outputs to Sentinel-2 MSI information grids, which geolocates data to a shared spatial grid and makes the use of satellite virtual constellations easier.

g. Conversion to dB

The unit-free backscatter coefficient is transformed to dB with a logarithmic transformation as the last phase of the preprocessing method.

3.3 Residual-Attention UNet++

The overall architecture of the Residual-Attention UNet++, a combined neural network framework that we provide for the segmentation of images of glacial lakes, is shown in Figure 2. It incorporates the attention mechanism, residual unit, and UNet++'s advantages. The suggested model employs UNet++ as its foundational network architecture, which utilizes reworked skip paths to link the encoder and decoder networks. Dense convolution blocks were used to transfer the encoder network's feature map to the decoder network. As seen above, the encoder's feature graph semantic degree is near to the decoder's feature graph semantic level [22-25].

Before anything else, skip connection features to remove extraneous areas from the picture $x \in \mathbb{R}^{H \times W} \times C$ in addition to the feature map generated by the lower encoder blocks with Transformer $z \in \mathbb{R}^{H' \times W' \times C'}$ are fed into the AG as shown in Equation (1)

$$f_a = (\sigma(\varphi(\delta(\theta(x)) + \theta(z)))) \otimes x$$

where φ , δ , and θ stand for elementwise multiplication, σ for sigmoid activation functions, and signify linear transformations. The result is then entered into the channel attention algorithm after being joined with the feature map. Equation (2) illustrates and describes the specifics of channel attention.

$$f_{ai} = (\sigma(\text{MLP}(\text{AvgPool}(F)) + \text{MLP}(\text{MaxPool}(F)))) \otimes F$$

Afterwards, two convolutions are performed. Equation (3) represents the spatial normalization map created by the Transformer, and f_z represents the output of these two convolutions $W_s \in \mathbb{R}^{1 \times H \times W}$.

$$W_s = \text{softmax}\left(\frac{QK^T}{\sqrt{d_k}}\right)V$$

as seen in (4), are multiplied element by element.

$$f_{sz} = W_s \otimes f_z$$

The following is the formula for the skip pathway: $x^{i,j}$ signifies the output of node $X^{i,j}$, i points to the down-sampling layer in accordance with the encoder sub-network, while j points to the dense block's convolution layer along the skip route [26]. $x^{i,j}$ is amenable to computation using the following formula:

$$x^{t/} = \begin{cases} \mu\{x^{s-1,j}\}, & j = 0 \\ \mu\left\{\int_{k=0}^{j-1} \text{AG}(x^{\ell k}), T(x^{f+1,j-1})\right\}, & j > 0 \end{cases}$$

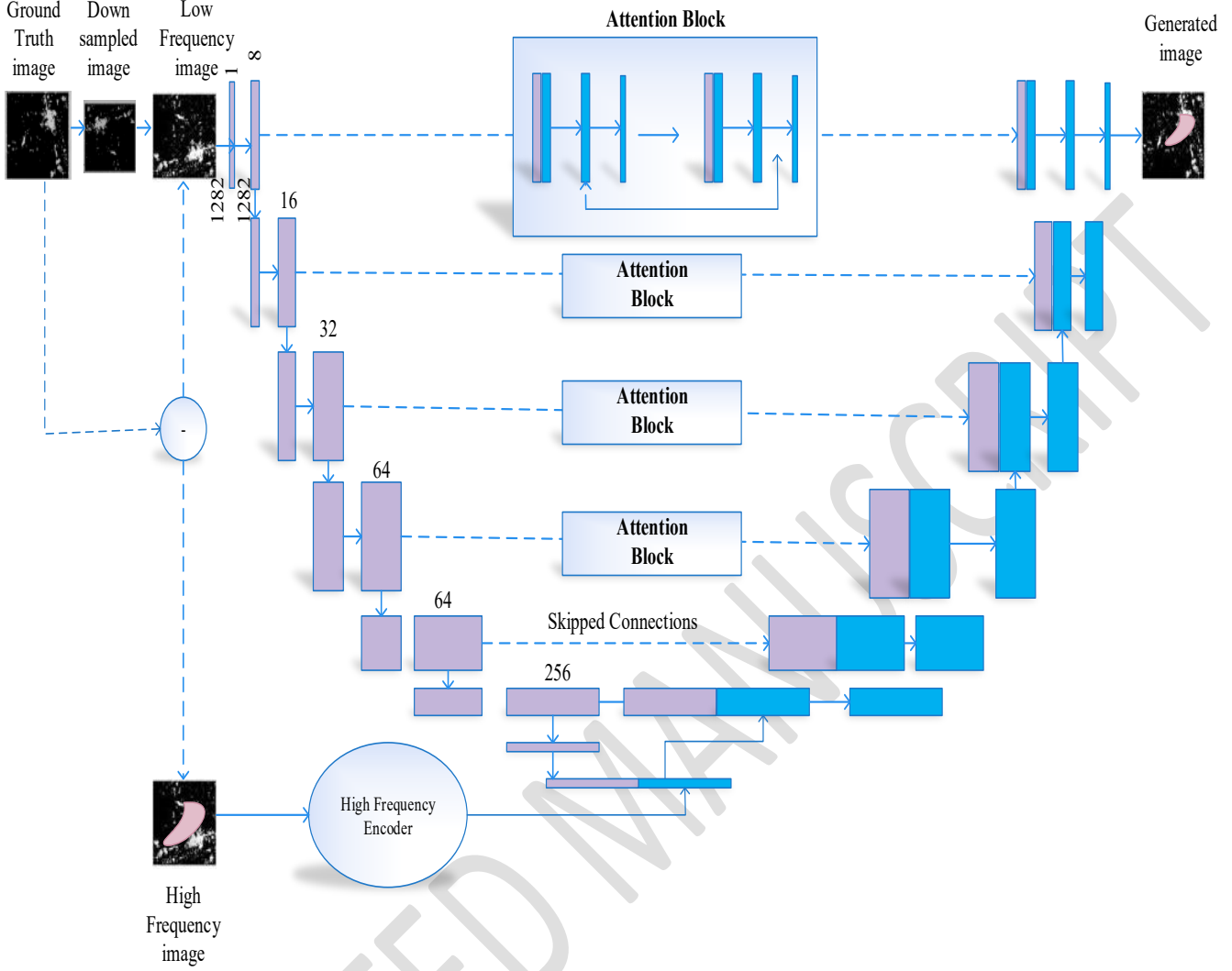


Figure 2 Structure of the Residual-Attention UNet++

function. This study used a multiclass form of the DC with cross-entropy algorithm as suggested in reference.

$$\ell_{\text{total}} = \lambda_1 \cdot \ell_{\text{Dice}} + \lambda_2 \cdot \ell_{\text{crossentropy}}$$

where λ_1 and λ_2 were equally set to 0.5:

- Cross-entropy loss:

$$\ell_{\text{crossentropy}}(u, y) = -\frac{1}{N} \sum_{c=1}^C \sum_{i=1}^N u_i^c \log y_i$$

u_i^c refers ground truth binary value N refers total amount of pixels, and C denotes classes Count. While y_i^c refers likelihood of segmentation that is projected to occur.

- Dice loss:

where $\mathcal{H}\{\cdot\}$ the concatenation layer, $\text{AG}(\cdot)$ stands for attention gate, $\text{T}(\cdot)$ for upsampling, and $[\cdot]$ for a convolution operation that follows a ReLU activation. The first skip route in Residual-Attention UNet++ is further explained in Figure 2. To guarantee fair comparisons with other methods, we used test photos for the test dataset and a random selection of samples for training for the training dataset. The performance gap between the suggested strategy and other models was evaluated using this random sampling methodology. Following the same approach as in, we used a weighted function that included both the DC and the cross-entropy loss [27]; the former is displayed in Equation (5), while the latter two are illustrated in Equations (6) & (7), respectively. It has been shown in other research as well that a compound loss function outperforms a single loss

$$\ell_{\text{Dice}}(u, y) = 1 - \frac{2 \sum_{c=1}^C \sum_{t=1}^N u_t^c y_t^c}{\sum_{c=1}^C \sum_{t=1}^N u_t^c + \sum_{c=1}^C \sum_{t=1}^N y_t^c}$$

3.4 Deep Supervision

Additionally, the proposed model incorporates deep supervision. To get feature maps at different semantic levels with complete resolution from $\{x^{\wedge}(0, j), j \in \{1, 2, 3, 4\}\}$, Residual-Attention UNet++ exploits dense skip connections in nested blocks. These feature maps may be efficiently monitored by an expert. We combined binary cross-entropy with dice coefficient to create the loss function [28] that we applied to each of the four nodes listed above:

$$\mathcal{L}(h, h) = -\frac{1}{N} \sum_{b=1}^N \left(\frac{1}{2} \cdot h_b \cdot \log h_b + \frac{2 \cdot h_b \cdot h_b}{h_b + h_b} \right)$$

where h_b and h_b the batch size, and represent the flatten predicted probability and flatten fundamental truths of the $b^{\wedge} \text{"th"}$ picture, respectively.

3.5 Super pixel segmentation technique

Asuperpixel segmentation technique, which has the benefits of a fast calculation process, strong edge matching, and a simple calculation procedure overall. To begin, it changes the picture format from RGB to CIELAB, where each pixel's coordinates (x , y) and color value (l , a , b) make up a five-dimensional vector V [l , a , b , x , y]. Then, using the concept of K means, an image is started with k superpixels and their distance is set as S . Calculating the exact center of these superpixels iteratively using a clustering algorithm is the fundamental portion. The CIELAB color space (d_c) and the geometry space (d_s) are both included in the dimension for five-dimensional vectors (D'). The distance may be determined using the following formulas:

$$\begin{aligned} d_c &= \sqrt{(l_j - l_i)^2 + (a_j - a_i)^2 + (b_j - b_i)^2}, \\ d_s &= \sqrt{(x_j - x_i)^2 + (y_j - y_i)^2}, \\ D' &= \sqrt{(d_c/m)^2 + (d_s/s)^2}, \end{aligned}$$

This stands for the greatest distance in CIELAB color space with the maximum value in geometric space, respectively. There is a 25×25 pixel searching range for every superpixel center. A pixel is allocated to the superpixel i center if its distance from its former center is smaller than the distance to the superpixel i center now. As long as the pixel distances to the fresh and prior superpixel centers stable, optimization continues in this iterative procedure. A rule-based fusion of semantic segmentation and SLIC segmentation is performed after iterating over the image's superpixel segmentation blocks. To start, find out how many superpixel pixels have multiple semantic segmentation labels. This superpixel segmented

block then has the semantic label containing extra pixels applied to each and every one of its pixels [29].

4. EXPERIMENTS AND RESULTS

The glacial lake area boundary is crucial for additional investigation and diagnosis. In order to demonstrate the efficacy of the Residual-Attention UNet++ approach, we ran experiments on Sentinel 2 true color scenes of High-Mountain Asia (HMA) region using glacial lakes inventory of this region. It covers an area of 2080.12 km² with nearly 30,121 glacial lakes. To create the Residual-Attention UNet++, a dataset of nearly 1000 and 2000 glacial lake images that covers lakes with different shapes, sizes and radiometric signatures. The model was trained for 200 epochs to reach stable convergence while avoiding overfitting. The optimizer was Stochastic Gradient Descent (SGD) with momentum because of its computational efficiency using large-scale image datasets. The learning rate was initially set to a value of 1e-4 and was gradually lowered as model performance improved over iterations. One dataset dealt with extraction, while the other showed cell nuclei segmentation from 2D pictures. Here, the PyTorch modules ran on a single GPU machine with 16 GB of RAM and an NVIDIA RTX 3070. While optimizing the model employing inertia and the stochastic gradient descent, its learning rate was gradually reduced throughout training. In the beginning, we set the following parameters: learning rate = 0.005, momentum = 0.9, and weight decay = 0.0001. The usage of adjustable learning rates was also used, with the rate of learning being reduced after a certain initial round count. The datasets were divided into training, validation, and test sets in a consistent approach considered to reduce potential bias in how the model evaluation is conducted and prevent overfitting. The training set included about 70% of the data. The validation dataset included 15% of the images and was used for the tuning process and the test set used for the final assessment of segmentation accuracy included 15% of the data.

4.1 Evaluation Metrics

Factors such as sensitivity (SE), F1-score, Intersection over Union (IoU), and dice coefficient (DC) were taken into account for the quantitative analysis of the experimental data. You can see the IoU calculation approach in Equation (4) and the SE calculation method in Equation (5).

$$\begin{aligned} \text{IoU} &= \frac{\text{TP}}{\text{TP} + \text{FN} + \text{FP}} \\ \text{SE} &= \frac{\text{TP}}{\text{TP} + \text{FN}} \end{aligned}$$

In Equation (6), the DC is shown.

$$\text{DC} = \frac{2|\text{GT} \cap \text{SR}|}{|\text{GT}| + |\text{SR}|}$$

The results of the UNet++ with Residual-Attention UNet++ evaluations on Glacial Lakes Extraction were shown in Figure 3. This data is organized as follows: first, the original picture; second, the ground truth; third, the output from UNet++; and finally, the output from Residual-Attention UNet++.

Residual-Attention UNet++ along with other algorithms' experimental performance on datasets is shown in Table 1.

Table 1. Methods Comparison

Methods	F1-Score	SE	IoU (%)	DC (%)
FCN	0.8318	0.8283	88.89	88.34
SegNet	0.8888	0.8888	89.94	81.40
U-Net	0.8441	0.8899	84.29	84.18
Attention UNet	0.8804	0.8048	88.19	88.81
UNet++	0.8923	0.8100	88.08	88.02
Attention UNet++	0.8928	0.8138	88.82	88.48
Residual Attention UNet++	0.9738	0.9788	98.48	98.41

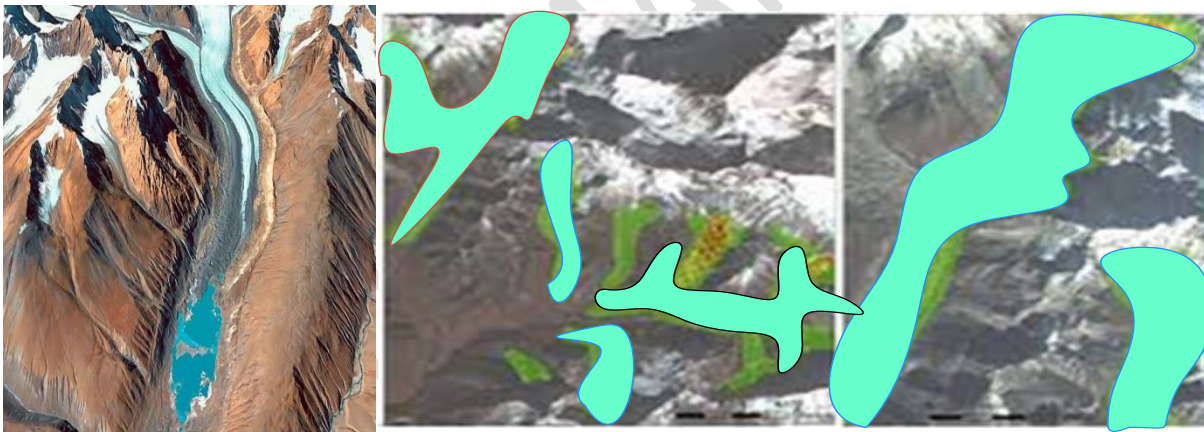


Fig. 3. Glacial Lakes Extraction

The suggested model's outstanding performance and resilience are further shown in Figure 4, which compares Residual-Attention UNet++ to other approaches on IoU after many tests. The proposed method surpasses the competition based on the segmentation accuracy and boundary delineation, regardless of the size or shape of the segments in the glacial lakes. In order to prevent misclassifications, the network was able to zero in on the most important characteristics with the aid of model-improved attention utilizing Residual-Attention UNet++. The segmentation job also benefited from Residual-Attention UNet++, which improved feature fusion among the decoder and the skip connections. Additionally, feature maps of various sizes worked together to promote deep supervision employing numerous side-outputs. When pictures are of varying sizes,

this leads to a more solid forecast. Lastly, optimizers find it simpler to solve the optimization issue between two encoders and decoders that are semantically comparable when dense skip connections are used. The optimizer's risk of being stuck at a local minimum is therefore reduced.

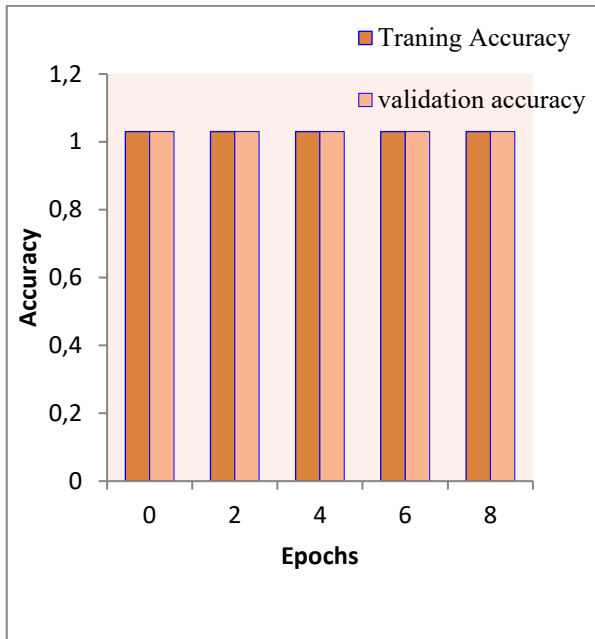


Fig 4. (a) Training and Testing Accuracy Comparison

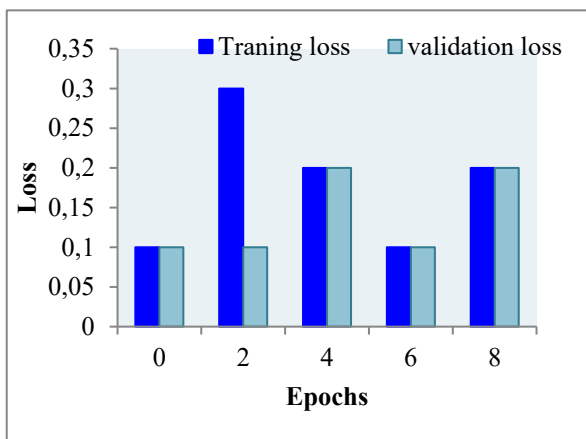


Fig 4. (b) Training and validation loss comparison

5. CONCLUSIONS

The proposed method utilizes remote sensing datasets for accurate extraction of glacial lakes. Current glacial lakes extraction algorithms cannot yet analyze bc and c + bc including features like spectral, shape, and texture characteristics, but rely on input parameters that require human designers to tune them. Hence, it is incapable of mining characteristics such as depth of glacial lakes using remote sensing photos with acceptable levels of precision. By comparison, the proposed Residual-Attention UNet++ achieved much higher levels of performance, with an F1-Score of 0.9738, Sensitivity of 0.9788, IoU of 98.48%, and Dice Coefficient of 98.41%. These outcomes surpass state-of-the-art models, UNet++, Attention UNet++, and SegNet when evaluating the same metrics among glacial lakes. This reinforces the model's capability and effectiveness for accurate glacial lake extraction compared to current

methods. There are constraints to the proposed framework, which include the need for large labelled datasets for training and possibly impracticalities in implementing real-time processing across large areas. Challenges to potential real-world deployment may consist of limited internet connectivity in remote mountainous areas, limited computing resources at local authorities, and early warning systems for susceptible communities. User-friendly as well as localized capacity building of stakeholders will be vital for practical uptake. The model performance may also vary as a result of the extreme terrain variability and influences of seasonal changes on backscatter. Future work will include the integration of multi-source data fusion from optical and thermal imagery to enhance detection accuracy. We also plan on expanding the model adaptability to other cryospheric regions around the globe. On an operational side, we will also develop near-real-time processing pipelines and cloud-based tools to enhance operational monitoring. Finally, ongoing research will utilize unsupervised learning and semi-supervised learning to minimize tom-foolery with the amount of required ground truth data.

REFERENCES

1. He, Y., Yao, S., Yang, W., Yan, H., Zhang, L., Wen, Z., Zhang, Y., & Liu, T. (2021). An Extraction Method for Glacial Lakes Based on Landsat-8 Imagery Using an Improved U-Net Network. *IEEE Journal of Selected Topics in Applied Earth Observations and Remote Sensing*, 14, 6544-6558.
2. Qu, G., Dai, X., Cheng, J., Li, W., Wang, M., Liu, W., Yang, Z., Shan, Y., Ren, J., Lu, H., Wang, Y., Zeng, B., & Atasoy, M. (2022). Characterization of Long-Time Series Variation of Glacial Lakes in Southwestern Tibet: A Case Study in the Nyalam County. *Remote. Sens.*, 14, 4688.
3. Yin, L., Wang, X., Du, W., Yang, C., Wei, J., Wang, Q., Lei, D., & Xiao, J. (2024). Using the Improved YOLOv5-Seg Network and Sentinel-2 Imagery to Map Glacial Lakes in High Mountain Asia. *Remote. Sens.*, 16, 2057.
4. Cao, Y., Pan, R., Pan, M., Lei, R., Du, P., & Bai, X. (2024). Refined glacial lake extraction in a high-Asia region by deep neural network and superpixel-based conditional random field methods. *The Cryosphere*.
5. Banerjee, P., & Bhuiyan, C. (2023). Glacial lakes of Sikkim Himalaya: their dynamics, trends, and likely fate—a timeseries analysis through cloud-based geocomputing, and machine learning. *Geomatics, Natural Hazards and Risk*, 14.
6. Dou, X., Fan, X., Wang, X., Fang, C., Lovati, M., & Zou, C. (2023). The response of glaciers and glacial lakes to climate change in the Southeastern Tibetan Plateau over the past three decades. *Land Degradation & Development*, 34, 5675 - 5696.
7. Murtem, R., Mandal, S., Nunchhani, V., Megozeno, M., Bandyopadhyay, A., & Bhadra, A. (2023). Temporal variation in glacier surface area and glacial lakes in

- glaciated river basins of Arunachal Pradesh. *Journal of Water and Climate Change*.
8. Cao, Y., Bai, X., Pan, M., Lei, R., & Du, P. (2023). Refined glacial lake extraction in high Asia region by Deep Neural Network and Superpixel-based Conditional Random Field.
 9. Zhao, H., Wang, S., Liu, X., & Chen, F. (2023). Exploring Contrastive Representation for Weakly-Supervised Glacial Lake Extraction. *Remote. Sens.*, 15, 1456.
 10. Wu, R., Liu, G., Zhang, R., Wang, X., Li, Y., Zhang, B., Cai, J., & Xiang, W. (2020). A Deep Learning Method for Mapping Glacial Lakes from the Combined Use of Synthetic-Aperture Radar and Optical Satellite Images. *Remote. Sens.*, 12, 4020.
 11. Nazakat, H., Hassan, S.N., Khan, G., ahmad, A., Qureshi, J.A., & Ali, S. (2021). Machine Learning Algorithms for Extraction of Glacial Lakes Using Ground Range Detected (GRD) Data: A Case Study from Hunza River Basin, Pakistan.
 12. Qayyum, N., Ghuffar, S., Ahmad, H.M., Yousaf, A., & Shahid, I. (2020). Glacial Lakes Mapping Using Multi Satellite PlanetScope Imagery and Deep Learning. *ISPRS Int. J. Geo Inf.*, 9, 560.
 13. Wangchuk, S., & Bolch, T. (2020). Enhancing alpine glacial lakes detection and mapping using multi-source data and machine learning techniques.
 14. Frey, H., Huggel, C., Allen, S.J., Emmer, A., Shugar, D.H., Farinotti, D., Huss, M., & Machguth, H. (2020). Towards a global assessment of future glacial lakes and related hazards, risks and opportunities.
 15. Ashraf, A., Iqbal, M.B., Mustafa, N., Naz, R., & Ahmad, B. (2021). Prevalent risk of glacial lake outburst flood hazard in the Hindu Kush–Karakoram–Himalaya region of Pakistan. *Environmental Earth Sciences*, 80.
 16. Yoon, D., Yu, H., & Lee, M. (2023). Detection of Floating Debris in the Lake Using Statistical Properties of Synthetic Aperture Radar Pulses. *GEO DATA*.
 17. Bhardwaj, D., Nagabhooshanam, N., Singh, A., Selvalakshmi, B., Angadi, S., Shargunam, S., ... & Rajaram, A. (2025). Enhanced satellite imagery analysis for post-disaster building damage assessment using integrated ResNet-U-Net model. *Multimedia Tools and Applications*, 84(5), 2689-2714.
 18. Xu, X., Liu, L., Huang, L., & Hu, Y. (2024). Combined use of multi-source satellite imagery and deep learning for automated mapping of glacial lakes in the Bhutan Himalaya. *Science of Remote Sensing*, 10, 100157.
 19. Shugar, D. H., Burr, A., Haritashya, U. K., Kargel, J. S., Watson, C. S., Kennedy, M. C., ... & Strattman, K. (2020). Rapid worldwide growth of glacial lakes since 1990. *Nature climate change*, 10(10), 939-945.
 20. Sahu, R., & Gupta, R. D. (2021). Spatiotemporal variation in surface velocity in Chandra basin glacier between 1999 and 2017 using Landsat-7 and Landsat-8 imagery. *Geocarto International*, 36(14), 1591-1611.
 21. Sunantha, O., Shao, Z., Pattama, P., Potchara, A., Huang, X., & Zeeshan, A. (2025). Machine learning-based estimation of soil organic carbon in Thailand's cash crops using multispectral and SAR data fusion combined with environmental variables. *Geo-spatial Information Science*, 1-23.
 22. Poloju, N., & Rajaram, A. (2024). Transformation with yolo tiny network architecture for multimodal fusion in lung disease classification. *Cybernetics and Systems*, 1-22.
 23. Lametti, A., Pichette, É., Ochs, C., Rajaram, A., Rayes, R., Cools-Lartigue, J., ... & Fiset, P. O. (2023). OA20. 06 Quantification of Pathologically Assessed Lymph Node Area in Lung Cancer Resection Using Deep Learning. *Journal of Thoracic Oncology*, 18(11), S92.
 24. Singh, A., Nagabhooshanam, N., Kumar, R., Verma, R., Mohanasundaram, S., Manjith, R., & Rajaram, A. (2025). Deep learning based coronary artery disease detection and segmentation using ultrasound imaging with adaptive gated SCNN models. *Biomedical Signal Processing and Control*, 105, 107637.
 25. Alagarsamy, M., Sakkarai, J., Mariappan, E., Malathi, K., Kamalam, G. K., Anthonisamy, A., ... & Rajaram, A. (2025). Dynamic Attention-Augmented Neural Network for Accurate and Efficient Brain Tumor Classification and Segmentation Using MRI. *International Journal of Pattern Recognition and Artificial Intelligence*, 2557005.
 26. Karthik, A., Hamatta, H. S., Patthi, S., Krubakaran, C., Pradhan, A. K., Rachapudi, V., ... & Rajaram, A. (2024). Ensemble-based multimodal medical imaging fusion for tumor segmentation. *Biomedical Signal Processing and Control*, 96, 106550.
 27. Babu, T., Selvanarayanan, R., Thanarajan, T., & Rajendran, S. (2024). Integrated early flood prediction using sentinel-2 imagery with VANET-MARL-based deep neural RNN. *Global NEST Journal*, 26(10).
 28. Karthik, S., Surendran, R., Kumar, G. V., & Srinivasulu, S. (2025). Flood prediction in Chennai based on extended elman spiking neural network using a robust chaotic artificial hummingbird optimizer. *GLOBAL NEST JOURNAL*, 27(4).
 29. Sundarapandi, A. M. S., Navaneethakrishnan, S. R., Hemlathadhevi, A., & Rajendran, S. (2024). A Light weighted dense and tree structured simple recurrent unit (LDTSRU) for flood prediction using meteorological variables. *Global NEST Journal*, 26(8).